富山大学水素同位体機能研究センター研究報告17：73－84，1997

論　文

トリチウム化メタンからのトリチウム回収に対する $Zr_{80}Ni_{20}$合金の適用性

松山政夫・本橋英一・舒　衛民・渡辺国昭

富山大学水素同位体機能研究センター
〒９３０－８５５５　富山市五福３１９０番地

Availability of $Zr_{80}Ni_{20}$-Alloy for Tritium Extraction from Tritiated Methane

Masao MATSUYAMA, Eiichi MOTOHASHI, W. M. SHU and Kuniaki WATANABE

Hydrogen Isotope Research Center, Toyama University
Gofuku 3190, Toyama 930-8555, Japan
(Received December 5, 1997; accepted March 9, 1998)

Abstract

Decomposition of methane by gettering materials is one of promising methods to extract tritium atoms from tritiated hydrocarbon species in the exhaust gases of thermonuclear fusion devices. Basic properties of the powered $Zr_{80}Ni_{20}$-alloy on the decomposition kinetics of methane and the absorption-desorption characteristics of hydrogen isotopes have been investigated. The $Zr_{80}Ni_{20}$-alloy mainly consisted of Zr and Zr_2Ni crystals. The decomposition rate obeyed the first order kinetics with respect to the pressure of methane, and most of metane(>99.7%) was decomposed within a few minutes at 723K. The activation energies for the decomposition were determined as 37.2 and 58.3 kJ/mol for temperatures of Region I and Region II, respectively. Pressure changes of hydrogen in the temperature range from 373 to 673K indicated the existence of two hydrides. ΔH° and ΔS° evaluated from temperature dependence of the equilibrium dissociation pressure at a low hydrogen concentration were determined as -168 kJ/mol-H_2 and -124J/K・mol-H_2, respectively. These values were close to those of Zr-hydride. On the other hand, the pressure changes at a high hydrogen concentration indicated the existence of Zr_2Ni-hydride. It was revealed, therefore, that hydrogen atoms liberated by methane decomposition are absorbed by Zr and Zr_2Ni crystals, depending on the hydrogen concentration in the $Zr_{80}Ni_{20}$-alloy.

1. Introduction

Most of the fuel injected into the reactor core of a fusion reactor is unburnt and exhaused by the vacuum system. The exhaust gas, however, containes impurities such as tritiated hydrocarbons and water vapor as well as oxygen, carbon monoxide and so on[1]. Therefore, it must be processed to recover tritium from the tritiated impurities. From the viewpoint of the best profitable use of fuel and the minimization of tritium waste, it is of great importance to extract tritium from tritiated impurity species. Tritium in the forms of tritiated methane and of water vapor could not be recovered by simple permeation method using the conventional palladium-silver membrane. Therefore, it is reqired to develop a basic technique to recover tritium.

Some techniques have been examined for this purpose; the following four candidate processes are actively underway at various tritium handling facilities[2-5].

(1) Hydrogen isotope permeation combined with hydrocarbon cracking by nickel catalyst at 753K and water decomposition through water gas shift reaction by zinc stabilized copper chromate catalyst at 473K.

(2) Combination of palladium membrane permeater with catalytic reactor, which is operated at 773K.

(3) High temperature isotopic exchange with swamping gas including hydrogen over platinum-on-alumina catalyst at 673K.

(4) Catalytic oxidation followed by high temperature vapor phase electrolysis.

On the other hand, hydrogen absorption alloys has been also proposed for processing methane which undergoes the slowest decomposition among the expected impurities[6-11]. Application of this method to the processing of tritiated impurities will bring about considrable simplification the processing system because of its simple operation principle. However, temperature around 873K is usually necessary for obtaining a required decomposition rate. The high temperature operation is not favorable to avoid tritium permeation through materials of the processing system.

Recently, it has been reported that Zr-Ni alloys are promising for the decomposition of methane[11-12]. It was found that the higher the Zr-content in the alloy is, the larger the decomposition rate is. For example, Zr_2Ni decomposed methane below 773K. This observation suggests that a Zr-Ni alloy having larger zirconium fraction is much usefull for

methane decomposition. In this study, we examined in detail the temperature dependence of the rate of methane decomposition and the absorption-desorption characteristics of hydrogen isotopes for $Zr_{80}Ni_{20}$-alloy.

2. Experimental

2.1. Apparatus

Figure 1 shows the schematic diagram of the experimental apparatus used for measuring methane decomposition and absorption/desorption kinetics of hydrogen isotopes. The apparatus consisted of high vacuum and measuring systems. These were mainly composed of an aluminum-alloy chamber, stainless steel tubes and metal bellows valves and a reaction vessel made of quartz. The high vacuum system consisted of a turbo molecular pump(TMP) backed with an oil-sealed rotary pump(RP), a sputter ion pump(SIP), a pressure gauge of Bayerd-Alpert type(B-A Gauge), and a quadrupole mass spectrometer(QMS). The residual pressure of the high vacuum system was routinely below $6x10^{-7}$ Pa. The residual gas was mainly hydrogen in addition to a small amount of water vapor and carbon monoxide.

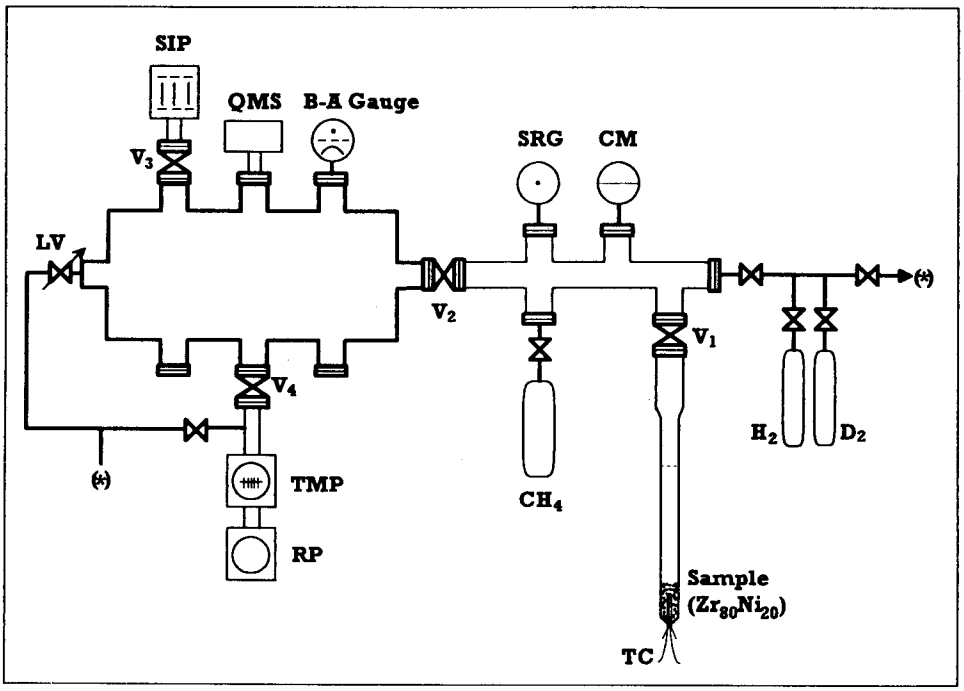

Fig. 1. Schematic diagram of the experimental apparatus

The measuring system consisted of pressure gauges, a reaction vessel, gas cylinders of methane, hydrogen and deuterium. Two kinds of pressure gauges, a spinning rotor gauge(SRG) and a capacitance manometer(CM), were used in the present study. The former gauge was used for measuring the methane decomposition rate and the equilibrium dissociation pressure of hydrogen isotopes for $Zr_{80}Ni_{20}$-hydride below 1 Pa, and the latter gauge was used for obtaining pressure-composition-temperature (P-C-T) curves of $Zr_{80}Ni_{20}$-hydride.

2.2. Materials

The sample used in the present study was $Zr_{80}Ni_{20}$-alloy, which was prepared from a mixture of each raw material with arch melting in argon atmosphere. The prepared alloy was powdered by absorption and desorption cycles of hydrogen before use in the reaction vessel. The amount of $Zr_{80}Ni_{20}$-alloy loaded into the reaction vessel was 1.77 g. The crystal structure of the powdered $Zr_{80}Ni_{20}$-alloy was analyzed by x-ray diffraction.

Hydrogen and deuterium were purchased from Nihon Sanso Co. The purity of each gas was 99.9999% and 99.6%, respectively. Methane was delivered from Takachiho Co., whose purity was 99%.

3. Results

3.1. Analysis of crystal structure of $Zr_{80}Ni_{20}$-alloy

Figure 2 shows the x-ray diffraction(XRD) pattern of the powdered $Zr_{80}Ni_{20}$-alloy. The XRD analysis was carried out after the powdered $Zr_{80}Ni_{20}$-alloy was degassed at 873 K in the reaction vessel. The XRD pattern showed many diffraction peaks, suggesting the formation of a plural crystal. In fact, most of the peaks observed

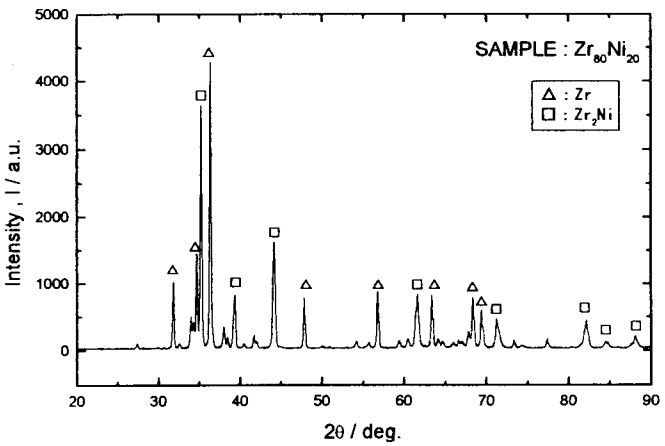

Fig. 2. X-ray diffraction pattern of the powdered $Zr_{80}Ni_{20}$-alloy.

were assigned to Zr and Zr_2Ni crystals. No diffraction peaks of nickel crystal were observed, although some unidentified peaks were remained.

3.2. Decomposition rate of methane

Figure 3 shows the observed time-course of the pressure decrease owing to methane decomposition in the temperature range from 423 to 723 K. The powdered $Zr_{80}Ni_{20}$-alloy was degassed at 873K for 1 hour prior to each decomposition reaction. The initial pressure of methane in each run was kept at 0.6 Pa, which corresponds to 1.20×10^{17} molecules-CH_4. The pressure decreased even at a low temperature of 423K. It was seen that over 99.7% of methane was decomposed within a few minutes at 723K, and most of hydrogen generated by methane decomposition was absorbed by the powdered $Zr_{80}Ni_{20}$-alloy. This indicates that $Zr_{80}Ni_{20}$-alloy has a high potential for methane decomposition and absorption of hydrogen generated. It shoud be noted that the pressure decreased exponentially with time at any temperature, indicating the first order kinetics with respect to methane pressure. The slope of each straight line, therefore, corresponds to the rate constant at a given temperature.

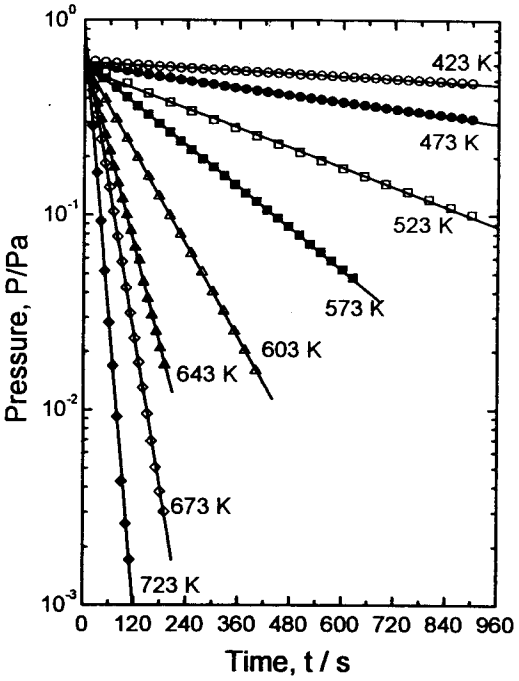

Fig. 3. Decomposition of methane in the temperature range from 423 to 723K.

The rate constants were plotted against the reciprocal of reaction temperature as shown in Fig. 4. The plot broke about 560K and could be divided into two regions, in each of which the plot gave a

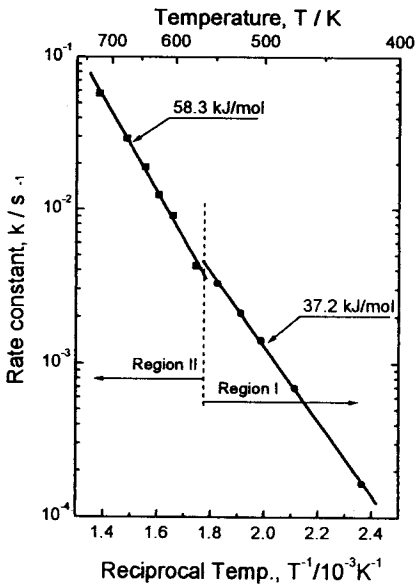

Fig. 4. Arrhenius plots of the rate constant of methane decomposition.

linear log k vs. 1/T relation. Hereafter, the region below 560K is called as "Region I", and that above 560K as "Region II". The activation energies can be evaluated from the ramps of those lines. They were determined as 37.2 and 58.3kJ/mol for Region I and Region II, respectively. Frequency factors were also estimated as 3.82×10^{-3} and 8.23×10^{-4} s^{-1}, respectively.

3.3. Absorption and desorption of hydrogen isotopes

A preliminary experiment in a high region of hydrogen concentration, which is denoted as n_H/n_M corresponding to the ratio of the number of absorbed hydrogen atoms to that of metal atoms, was carried out to examine the absorption and desorption character- istics of hydrogen by powdered $Zr_{80}Ni_{20}$-alloy. A given amount of the $Zr_{80}Ni_{20}$-alloy was loaded into the reaction vessel and it was degassed at 773K. After that, it was cooled to 373K, where the residual pressure was below 1.0×10^{-6}Pa. Subsequently, a given amount of hydrogen(3.16×10^{-2} mol-H_2: n_H/n_M=3.02) was introduced into the reaction vessel. After the hydrogen pressure reached a steady state, the $Zr_{80}Ni_{20}$-alloy was heated stepwise up to 673K, and again cooled down to 373K in the same manner.

Figure 5 shows an example of pressure change with temperature. The open and closed circles represent heating and cooling processes, respectively. At 373K, the amount of hydrogen absorption was evaluated as 1.50×10^{-2} mol from the remaining gas pressure. It was seen that about 50% of loaded hydrogen was absorbed. In addition, n_H/n_M was calculated as $(Zr_{0.8}Ni_{0.2})H_{1.43}$ at 373K and $(Zr_{0.8}Ni_{0.2})H_{1.08}$ at 673K. On the other hand, two

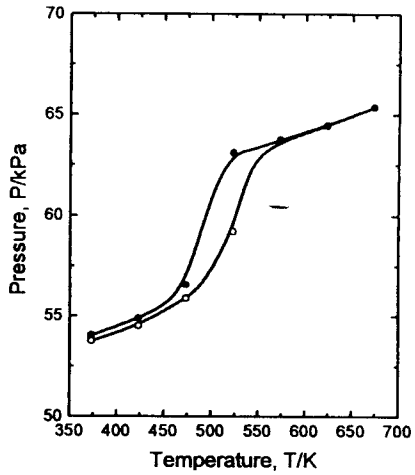

Fig. 5. An example of pressure change with temperature.

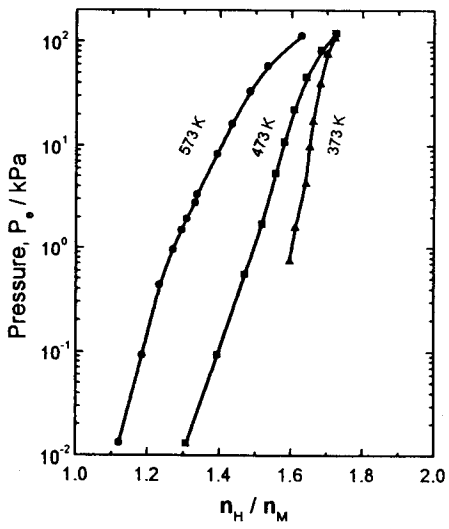

Fig. 6. P-C-T curves for $Zr_{80}Ni_{20}$-hydride.

plateau regions were observed within the temperature region studied. This indicates that $Zr_{80}Ni_{20}$-hydride has two different hydride phases.

Figure 6 shows the P-C-T curves in the high concentration region at 373, 473 and 573K. It is clearly seen that the equilibrium dissociation pressure of $Zr_{80}Ni_{20}$-hydride increased steeply with increasing hydrogen concentration. Although no clear plateau with hydride formation was observed within the present experimental conditions, the P-C-T curves indicate that hydrogen absorbed formed a quite stable hydride phase.

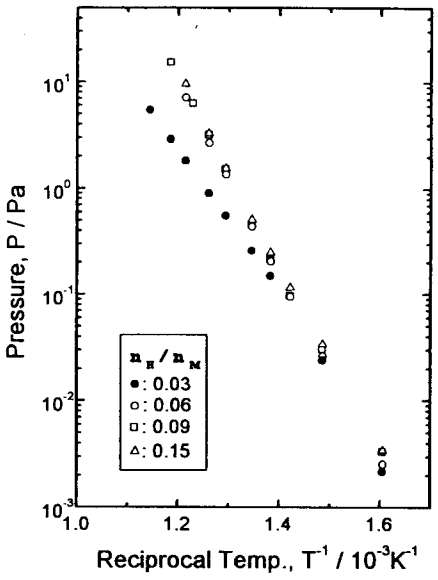

Fig. 7. Temperature dependence of the equilibrium dissociation pressure of hydrogen in the concentration range from 0.03 to 0.15.

On the other hand, to examine the absorption and desorption characteristics of hydrogen in a low concentration, the temperature dependencies were examined at the hydrogen concentrations of 0.03, 0.06, 0.09 and 0.15. Figure 7 shows the temperature dependence of the equilibrium dissociation pressure of hydro- gen. The plot resulted in a straight line regardless of the hydrogen concentration except 0.03. In the case of 0.03, the data points lay in the straight line below about 700K, whereas above 700K different temperature dependence appeared. This indicates that a different absorbed state of hydrogen exists in low hydrogen concentration below 0.03.

Thermodynamic data for hydrogen absorption evaluated from Fig. 7 are summarized in Table 1. Below 700K, the standard enthalpy and the entropy changes, ΔH° and ΔS°, were determined as -168 ± 1 kJ/mol-H_2 and -124 ± 2 J/K · mol-H_2, respectively. These values were independent on hydrogen con- centration, and were close to those for Zr-hydride as presented

Table 1. Summary of thermodynamic data of hydride formation on $Zr_{80}Ni_{20}$-alloy.

n_H/n_M	$-\Delta H^\circ$ (kJ/mol(H_2))	$-\Delta S^\circ$ (J/K · mol-H_2)	Remarks
0.03	167	121	<700 K
	125	62	>700 K
0.06	169	125	-----
0.09	169	126	-----
0.15	168	125	-----

later. However, those became much small above 700K in the concentration of 0.03: namely, the values of ΔH° and ΔS° were evaluated as -125 kJ/mol-H_2 and -62 J/K · mol-H_2, respectively.

Figure 8 shows the temperature dependence of equilibrium dissociation pressure for deuterium. In this experiment, deuterium concentration was set at n_D/n_M=0.06. To make the isotopic effect clear corresponding hydrogen data are presented together. It can be clearly seen that deuterium also gives a good straigh line, from which thermodynamic data, ΔH° and ΔS°, were determined as -170 kJ/mol-D_2 and -129 J/K · mol-D_2, respectively. These values are slightly larger than those of $Zr_{80}Ni_{20}$-hydride. This indicates that there is little isotope effect on the dissociation pressure of hydrogen isotopes, suggesting that tritium will show similar temperature dependence.

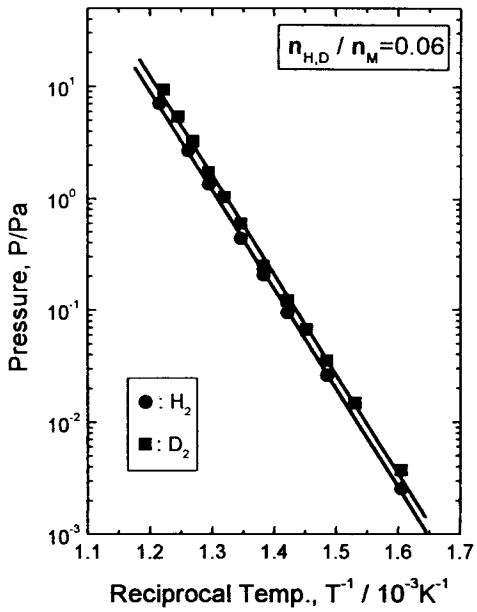

Fig. 8. Temperature dependence of the equilibrium dissociation pressures of $Zr_{80}Ni_{20}$-hydride and -deuteride.

4. Discussion

4.1. Decomposition reaction of methane

The specific surface area of the alloy powder was determined to be 0.2 m^2/g by means of BET method. This means that the net surface area of the sample was 0.354 m^2, and hence the number of surface sites is estimated to be 3.5×10^{18} by assuming that the surface site density is 1×10^{19} m^{-2} [13]. On the other hand, the amount of methane used was 1.2×10^{17} molecules. Namely, the surface coverage should not exceed 0.03 even if all of the methane introduced is adsorbed on the surface. The coverage is so small that the reaction kinetics is hardly affected by the presence of adsorbed methane and its decomposition residue. This is supported by the fact that the plots of log p vs. t showed good linear lines over 99% decomposition.

There are a number of observations on the adsorption of methane on metals such as Ti, Ta, Cr, Mo, W, Rh and Pd[14]. The adsorption and decomposition of methane on evaporated nickel film was studied by Wright et al.[15], who reported that the adsorption of methane becomes rapid and slow liberation of hydrogen begins at 413K. It is also noted that adsorption species on nickel are considered to be CH_2 radical at 423K and CH radical at 473K. In both the cases, the decomposition of methane obeys the first order kinetics. Those observations agree well with the present results.

In each run, all of hydrogen atoms generated by the methane decomposition appeared to be instantaneously absorbed in the $Zr_{80}Ni_{20}$-alloy. One of the reason is that the hydrogen concentration in the alloy is extremely low even though all of hydrogen atoms are absorbed. According to Wright et al.[15], the rate-limiting step in the decomposition of methane is the breakdown of methyl radicals formed on the surface of evaporated nickel. This appears to be valid for the present observations, and hence it is likely concluded that the rate-limiting step is the breakdown of methyl radicals, where the CH_2 radical plays a role for Region I and the CH radical for Region II.

Concerning to activation energy of methane decomposition, Emerson et al. obtained 59.3 $\pm$3.5 kJ/mol in a temperature range from 673 to 913K for St. 101(Zr-Al getter)[16]. In addition, Hobson's data for methane decomposition by St. 707(Zr-V-Fe getter) in a temperature range from 363 to 673K[17] show similar break in log p vs. 1/T plot, giving comparable activation energies to those evaluated for Region I and Region II. Namely, three different alloys($Zr_{80}Ni_{20}$(Zr+Zr_2Ni), Zr-Al and Zr-V-Fe) exhibit a very similar feature on the activation process. This implies that zirconium atoms on the alloy surface play an important role for methane decomposition.

In other words, the diffusion of carbon does not play a role in the present case, which will require much higher activation energy:128 kJ/mol is reported for α-Zr[18]. It shoud be noted here, however, that the rate-limiting step will change with increasing carbon coverage because of the large activation energy for diffusion

4.2. Absorption and desorption behavior of hydrogen isotopes

A feature of the plural crystalline nature of the sample alloy appeared in the pressure changes with temperature as shown in Fig. 5. ΔH° and ΔS° for Zr-hydride formation were reported as -188 kJ/mol-H_2 and -143 J/K · mol-H_2, respectively[19]. As for Zr_2Ni-deuteride,

they were reported as -72 kJ/mol-D_2 and -138 J/K · mol-D_2, respectively[20]. From these thermodynamic data, the dissociation pressures of Zr- and Zr_2Ni-hydride can be estimated at various temperatures by assuming that the temperature dependence on dissociation pressure of Zr_2Ni-hydride is little different from that of deuteride as being discussed below. For example, the dissociation pressures of Zr-hydride at 373K and 673K are calculated as $1.3x10^{-14}$ and $7.3x10^{-3}$ Pa, respectively. On the other hand, those for Zr_2Ni-hydride at the same temperatures are calculated as $1.4x10^{2}$ and $4.3x10^{6}$ Pa, respectively. The latter are remarkably higher than the former. This indicates that Zr-hydride in the $Zr_{80}Ni_{20}$-alloy does not contribute to the pressure increase with temperature rise. Namely, the pressure change observed in Fig. 5 is due to the dissociation of Zr_2Ni-hydride.

According to the thermodynamic data for Zr_2Ni-deuteride by Watanabe et al.[20], P-C-T curves does not show a plateau region in a concentration range from $Zr_2NiD_{0.09}$ to $Zr_2NiD_{3.5}$. Although the fraction of Zr_2Ni crystal in the $Zr_{80}Ni_{20}$-alloy used has not been determined, steep pressure changes in the P-C-T curves in Fig. 6 are consistent with the characteristics of Zr_2Ni-deuteride mentioned above. Such a steep pressure change is favorable for the processing of tritiated methane and water vapor to recover tritium efficiently from $Zr_{80}Ni_{20}$-tritide.

Temperature dependence of the dissociation pressure in a low concentration region was examined as shown in Fig. 7. Values of the thermodynamic data obtained were close to those for Zr-hydride described previously. Namely, this indicates that most of hydrogen liberated by methane decomposition is absorbed into zirconium as the hydrogen concentration in the $Zr_{80}Ni_{20}$-alloy is low. If the $Zr_{80}Ni_{20}$-alloy is applied to the decomposition of tritiated methane, the dissociation pressure of tritium should be lowered up to the $Zr_{80}Ni_{20}$-tritide formation of a high concentration. Therefore, the tritium absorbed by zirconium may be inventory of a tritium extraction device. To lower the tritium inventory, it is of a great important subject to prepare $Zr_{80}Ni_{20}$-alloy which consists of a small fraction of Zr.

5. Conclusions

Tritium in impurity gases such as tritiated hydrocarbons and water vapor mixed in the exhaust gas of the reactor core of a thermonuclear fusion device must be extracted from the

viewpoints of the best profitable use of tritium and of the decrease of tritium waste. Methane is hardly decomposed in tritiated impurities. Decomposition by getter materials is one of promising methods for above purpose. From this viewpoint, basic properties of the powered $Zr_{80}Ni_{20}$-alloy on the decomposition kinetics of methane and the absorption- desorption characteristics of hydrogen isotopes were investigated.

It was clarified by x-ray diffraction analysis that the $Zr_{80}Ni_{20}$-alloy used in the present study mainly consisted of two constituents of Zr and Zr_2Ni crystals. The decomposition rate obeyed the first order kinetics with respect to the pressure of methane and over 99.7% of metane was decomposed within a few minutes at 723K. The temperature dependence of the rate constants of decomposition reaction did not show a linear line; that is, the discontinuity of the temperature dependence appeared around 560K(below this temperature is called as Region I, while above this temperature is called as Region II). The activation energies were determined as 37.2 and 58.3 kJ/mol for Region I and Region II, respectively.

Pressure change in a temperature range from 373 to 673K indicated the existence of two hydrides. Thermodynamic data, ΔH° and ΔS°, evaluated from temperature dependence of the equilibrium dissociation pressure at a low hydrogen concentration were determined as -168 kJ/mol-H_2 and -124J/K · mol-H_2, respectively. These values were close to those of Zr-hydride. On the other hand, the pressure changes with a temperature change in a high hydrogen concentration indicated the existence of Zr_2Ni-hydride which shows a remarkably higher dissociation pressure than Zr-hydride. It is revealed, therefore, that hydrogen liberated by decomposition is absorbed by Zr and Zr_2Ni, depending on the hydrogen concentration in $Zr_{80}Ni_{20}$-alloy. This is also true for tritiated methane.

From these results, it was revealed that the $Zr_{80}Ni_{20}$-alloy has a high potential for extraction of tritium from tritiated methane in the exhaust gas. This alloy will be also applicable to the decomposition of tritiated water vapor, because it is easy to decompose water vapor than methane.

References

1) J. Koonce, H. Yoshida, O. Kveton, H. Horikiri and R. Haange, Fusion Technol., **28** (1995) 630.

2) R. Haange, H. Yoshida, O. Kveton, J. Koonce and H.Horikiri, Fusion Technol., **28** (1995) 491.

3) J.M. Miller, L. Rodrigo and J.A. Senohrabek, Fusion Technol., **28** (1995) 700.

4) R.-D. Penzhorn and M. Glugra, Proc. Int. Tritium Workshop on Present Status and Prospect of Tritium Material Interaction Studies, Kuroda Kohodo, Toyama Univ., July 18-19, (1996) p. 17.

5) A.N. Perevezentsev and J.L. Hemmerich, Proc. Int. Tritium Workshop on Present Status and Prospect of Tritium Material Interaction Studies, Kuroda Kohodo, Toyama Univ., July 18-19, (1996) p. 29.

6) E. Willin, M. Sirch, R.-D. Penzhorn and M. Devillers, Fusion Technol., **14** (1988) 756.

7) R.-D. Penzhorn, M. Devillers and M. Sirch, J. Nucl. Mater., **170** (1990) 217.

8) U. Tamm, E. Hutter, G. Neffe and P. Schira, Fusion Technol., **21** (1992) 983.

9) W.T. Shmayda, N.P. Kherani, B. Wallace and F. Mazza, Fusion Technol., **21** (1992) 616.

10) J.D. Baker, D.H. Meikrantz, R.J. Pawelko and R.A. Anderl, J. Vac. Sci. Technol., **A12** (1994) 548.

11) W.M. Shu, M. Matsuyama and K. Watanabe, Ann. Rept. Hydrogen Isotope Research Center, Toyama Univ., 16 (1996) 59.

12) K. Watanabe, W.M. Shu, E. Motohashi and M. Matsuyama, Poc. 4th Int. Symp. on Fusion Nuclear Technology, Meiji Kinenkan, Tokyo, (1997), in press.

13) J.R. Andreson, "Structure of Metallic Catalysts", Academic Press, London, (1995), p. 296.

14) B.M.W. Trpnell, Trans. Fraday Soc., **52** (1956) 1618.

15) P.G. Wright, P.G. Ashmore and C. Kemball, Trans. Faraday Soc., **54** (1958) 1692.

16) L.C. Emmerson, R.J. Knize, J.L. Cecchi and O. Auciello, J. Vac. Sci. Technol., **A4** (1986) 297.

17) J.P. Hobson and R. Chapman, J. Vac. Sci. Technol., **A4** (1986) 300.

18) The Japan Institute of Metals ed., "Kinzoku Data Book", Maruzen, Tokyo, (1986), p. 29.

19) E.A. Gulbransen and K.P. Andrew, Trans. Met. Soc., AIME, **203** (1955) 136.

20) K. Watanabe, K. Tanaka, M. Matsuyama and K. Hasegawa, Fusion Eng. Design, **18** (1991) 27.